NIH Public Access
Author Manuscript
Neuroimage. Author manuscript; available in PMC 2011 February 15.

Published in final edited form as:
Neuroimage. 2010 February 15; 49(4): 3230. doi:10.1016/j.neuroimage.2009.11.047.

Predicting Grip Force Amplitude Involves Circuits in the Anterior Basal Ganglia

Pooja Wasson[1], **Janey Prodoehl**[1], **Stephen A. Coombes**[1], **Daniel M. Corcos**[1,2,3,5], and **David E. Vaillancourt**[1,2,4]

[1]Department of Kinesiology and Nutrition, University of Illinois at Chicago, Chicago, IL

[2]Department of Bioengineering, University of Illinois at Chicago, Chicago, IL

[3]Department of Physical Therapy, University of Illinois at Chicago, Chicago, IL

[4]Department of Neurology and Rehabilitation, University of Illinois at Chicago, Chicago, IL

[5]Department of Neurological Sciences, Rush University Medical Center, Chicago, IL

Abstract

The ability to grip objects allows us to perform many activities of daily living such as eating and drinking. Lesions to and disorders of the basal ganglia can cause deficits in grip force control. Although the prediction of grip force amplitude is an important component of performing a grip force task, the extant literature suggests that this process may not include the basal ganglia. This study used functional magnetic resonance imaging (fMRI) to explore the functional brain mechanisms underlying the prediction of grip force amplitude. The mean force and duration of force did not vary across prediction levels. As anticipated, the reaction time decreased with the level of grip force predictions. In confirmation of previous studies, the parieto-frontal and cerebellar circuits increased their fMRI signal as grip force predictability increased. In addition, the novel finding was that anterior nuclei in the basal ganglia such as caudate and anterior putamen also had an fMRI signal that increased with the level of grip force prediction. In contrast, the fMRI signal in posterior nuclei of the basal ganglia did not change with the level of prediction. These findings provide new evidence indicating that anterior basal ganglia nuclei are involved in the predictive scaling of precision grip force control. Further, the results provide additional support for the planning and parameterization model of the basal ganglia by demonstrating than specific anterior nuclei of the basal ganglia are involved in planning grip force.

Introduction

The ability to grip objects allows us to perform many activities of daily living such as eating and drinking. When we lift an object there is a parallel increase in grip force and load force before lift off (Forssberg et al., 1991; Johansson and Cole, 1994). Since explicit information about the weight of an object is available only at lift off, individuals use visual information of the object's properties to predicatively scale appropriate fingertip forces (Danion and Sarlegna,

© 2009 Elsevier Inc. All rights reserved.

Corresponding Author: David E. Vaillancourt, PhD University of Illinois at Chicago 1919 West Taylor 650 AHSB, MC 994 Chicago, IL 60612 312-355-2058 court1@uic.edu.

Publisher's Disclaimer: This is a PDF file of an unedited manuscript that has been accepted for publication. As a service to our customers we are providing this early version of the manuscript. The manuscript will undergo copyediting, typesetting, and review of the resulting proof before it is published in its final citable form. Please note that during the production process errors may be discovered which could affect the content, and all legal disclaimers that apply to the journal pertain.

NIH-PA Author Manuscript
NIH-PA Author Manuscript
NIH-PA Author Manuscript

NIH-PA Author Manuscript

NIH-PA Author Manuscript

NIH-PA Author Manuscript

2007; Flanagan et al., 2001; Gordon et al., 1991a, b). Despite the fact that visual information allows predictive grip force scaling, relatively little is known about the neuronal processes in the brain that mediate our ability to predict an appropriate grip force output.

Predicting an appropriate grip force output is an important component of the planning process. Schmitz and colleagues (2005) studied brain activity during predictable and unpredictable weight changes during a grip force task that did not use visual feedback. During predictable grip force, they found increased brain activity in parietal-frontal circuits, along with the left cerebellum and left thalamus. While scanning coverage included the basal ganglia nuclei, they did not find any changes in activation in the basal ganglia. However, there is emerging evidence to suggest that the basal ganglia are involved in grip force control.

In a recent review on precision grip force control (Prodoehl et al., 2009), the basal ganglia have been proposed to regulate specific aspects of precision grip force control. For instance, the planning and parameterization model of the basal ganglia proposes that anterior nuclei (eg. caudate and anterior putamen) in the basal ganglia are involved in planning grip force, and posterior nuclei (eg. subthalamic nucleus and internal globus pallidus) in the basal ganglia are involved in the parameterization of grip force output (Prodoehl et al., 2009). In support of this model, subjects were asked to produce grip force that was either at a consistent force amplitude level or was deliberately varied by the subject to internally select different force amplitudes (Vaillancourt et al., 2007). Using fMRI to examine activation in the basal ganglia, the authors found that the anterior basal ganglia nuclei showed increased activation related to the selection component of the task whereas activation in posterior basal ganglia nuclei was related to dynamic force pulse production. Pope and colleagues (2005) used a slightly different force production task and also found a specific role for anterior basal ganglia nuclei in planning and switching aspects of force control. It remains unclear however if anterior basal ganglia nuclei, which include the caudate and anterior putamen, have a role in the prediction of grip force output.

The purpose of this study was to use functional magnetic resonance imaging (fMRI) to examine how the blood oxygen level dependent (BOLD) signal changes during a grip force task that utilized different levels of predictability of appropriate force amplitude. The independent variable manipulated was the number of predictable force pulses during a sequence of grip force pulses. We expected that when subjects could predict the amplitude of the upcoming force pulse their reaction time would decrease (Hick, 1952; Hyman, 1953). Since it has been shown that the amplitude of force and duration of force can both affect BOLD fMRI signals in the basal ganglia (Prodoehl et al., 2008b; Spraker et al., 2007), these parameters were carefully controlled across prediction levels. Based on the planning and parameterization model (Prodoehl et al., 2009), we test the hypothesis that the caudate and anterior putamen are part of the parietal-frontal and cerebellar circuits that have previously been shown to be involved in grip force prediction. We also test the hypothesis that other nuclei in the basal ganglia (such as subthalamic nucleus and globus pallidus) will not show increased activity when the number of predictable force pulses increases.

Methods

Subjects

Eleven neurologically healthy right handed subjects (5 males and 6 females) age 21-33 years participated in the experiment. All subjects agreed to the experimental procedure by giving informed consent. The research plan was approved by the local Institutional Review Board and all procedures were in compliance with the Declaration of Helsinki.

NIH-PA Author Manuscript

NIH-PA Author Manuscript

NIH-PA Author Manuscript

Force Data Acquisition

Subjects produced force on a rigid precision grip device with the index and middle finger opposing the thumb of their right hand. The custom made pinch grip device (Vaillancourt et al., 2003) was made of non metallic material (polycarbonate) and was therefore suitable for use within the fMRI environment. The pinch grip device was connected to a 35 feet long plastic tube which loaded into an Entran (EPX-NI3-250P) pressure transducer located outside the fMRI environment. When force was produced against the pinch grip device, hydraulic pressure increased. This increase was sensed by the pressure transducer. The output of the pressure transducer was amplified through a pressure gauge amplifier. A PCMCI National Instruments A/D converter sampled the pressure at 100 Hz. The subject was presented with online visual feedback of the force produced.

MRI Data Acquisition

Magnetic resonance images were collected using a volume head coil inside a 3 Tesla MR Scanner (GE Healthcare 3T94 Excite 2.0). To minimize any head movement, foam pads were fitted around the head of the subject. In addition, visual feedback about head position was provided to the subject through the use of a projector-visor system (Thulborn and Shen, 1999). The subject's ears were shielded from the noise of the scanner with the use of earphones and earplugs. The functional images were collected with a T_2* sensitive, single-shot, gradient-echo echo-planar pulse sequence (echotime 25 ms; repeat time 2500 ms; flip angle 90; field of view 200 mm; imaging matrix 64 × 64; 42 contiguous slices with a slice thickness of 3mm). Slices were acquired axially with full coverage of the brain including the cerebellum. Following the fMRI scans, anatomical images were collected using a T1 weighted 3D inversion recovery fast spoiled gradient recalled (3DIRfSPGR) pulse sequence (echotime 3 ms; repeat time 25 ms; flip angle 40; field of view 240 mm; imaging matrix 256 × 256; 120 contiguous slices with a slice thickness of 1.5 mm).

Experimental Design

The maximum voluntary contraction (MVC) was collected first as subjects were asked to sustain a maximum force for three consecutive 5s trials. Each trial was separated by a period of rest. The MVC was calculated as the average force during the sustained force period. The fMRI experiment was performed as a block design, with a total of 3 separate fMRI scans. As depicted in Figure 1A, each of the functional scans consisted of a 30s rest period alternating with a 30s task block that repeated 4 times and ended with an additional rest period.

Subjects were positioned supine in the scanner, and held the pinch grip device in their right hand. During the 30s rest period subjects could see on a display screen two horizontal bars: a white cursor bar and a target bar (above the white bar). The target bar was red, and both the white cursor bar and the red target bar were stationary. During the rest time subjects were instructed to fixate on the stationary target bar and produce no force.

During each 30s task block, subjects were required to produce two sequences of 5 force pulse contractions (i.e. sequence of pulses 1-5 and sequence of pulses 6-10). To cue the initiation of the first force pulse of a sequence the target bar turned to blue from red and simultaneously reached a target force level on screen (Figure 1B – Pulse 1). Upon seeing this cue, the subject initiated force production to match the white cursor bar to the displayed target force bar. The white cursor bar was directly related to the force produced by the subject and moved vertically towards the target bar with an increase in force. The target bar stayed at the particular force level for a period of 2s after which it returned to red for 1s. This served as the cue for the subject to relax by stopping force production. To cue the initiation of each of the following force pulses, the target bar turned to green (not blue) from red and simultaneously reached a target force level on screen (Figure 1B – Pulses 2-5 and Pulses 7-10). For each of these force pulses, the

NIH-PA Author Manuscript

NIH-PA Author Manuscript

NIH-PA Author Manuscript

target force level was displayed for a period of 2s and was followed by a red target bar for 1s. Once the target bar cue was available, subjects were instructed to respond quickly and produce each force pulse as fast and accurately as possible. The target force levels were set to different percentages of the subject's MVC based on a set of prediction rules.

The three functional scans measured three levels of predictability: 20%, 40% and 80%. The 20% level of predictability was the least predictable and the 80% level of predictability was the most predictable. (1) 20% (Figure 1B): Subjects were trained in advance that within each force sequence of the task block, the target force level for the second pulse of each five pulse sequence would be at the same force level as the first pulse of that sequence. This is shown in Figure 1B where the target force level for pulse 2 is at the same force level as for pulse 1 and the target force level for pulse 7 is at the same force level as for pulse 6. Thus, pulses 2 and 7 were predictable. The target force levels for pulse 1 and pulse 6 could appear at any force level and therefore were unpredictable for the subjects. Similarly, the target force levels for pulses 3, 4, 5, 8, 9 and 10 could appear at any force level and were also unpredictable for the subjects. (2) 40% (Figure 1C): Similar to the 20% level of predictability, subjects were trained in advance that within each force sequence of the task block, the target force level for pulse 2 would be at the same force level as pulse 1, and pulse 7 at the same force level as pulse 6. In addition, subjects were trained that the force level for pulse 3 would be at double the force level of pulse 1, and pulse 8 would be double the force level of pulse 6. (3) 80% (Figure 1D): Similar to the 40 % level of predictability, subjects were trained in advance that within each force sequence of the task, the target force level for pulse 2 would be the same as pulse 1, and pulse 7 the same as pulse 6. In addition, consistent with the 40% level of predictability pulse 3 was double that of pulse 1, and pulse 8 was double that of pulse 6. In addition, they were trained that the target force level for pulse 4 would be half the force level of pulse 1 of the sequence, and pulse 9 would be half that of pulse 6. Finally, the target force level for pulse 5 would be 75% greater than pulse 1, and pulse 10 would be 75% greater than pulse 6.

Subjects were trained extensively for two hours outside the scanner on the day before fMRI data collection so that the subjects learned the rules to apply within the three levels of predictability of the scans. When in the scanner, subjects were informed before each scan about the level of predictability in the upcoming scan and the order of the 3 scans was counterbalanced across subjects. It is important to note that the values of the target force levels were not identical for the two force sequences within a task block. For instance in the 20% level of predictability, one of the task blocks had the following target force levels: 5, 5, 10, 14, and 20 % of MVC for sequence of pulses 1-5, and 18, 18, 30, 22 and 8% of MVC for sequence of pulses 6-10, respectively. Additionally, no two force sequences were identical across the task blocks. This was done to ensure that the subject was making active use of the information provided by the first target force level to predict the force level of the upcoming pulse in each and every forthcoming sequence.

Further, since previous studies have shown that the cortex and specific nuclei in the basal ganglia (subthalamic nucleus and internal segment of the globus pallidus) increase in signal intensity with the average level of force output during a grip task (Dai et al., 2001; Spraker et al., 2007), the average of the target force levels that were displayed during a single task block of any scan was kept constant at 15% of MVC. Therefore the average force produced across the three scans was controlled. A low value of 15% of MVC was chosen to minimize the effects of fatigue during task performance.

Force and fMRI Data Analysis

Force data analysis—The reaction time for each force pulse in every task block of the three levels of predictability was calculated using a custom written algorithm in MATLAB. The mean force during each force pulse was calculated during the steady-state phase of the 2s pulse.

NIH-PA Author Manuscript

NIH-PA Author Manuscript

NIH-PA Author Manuscript

The mean force was then averaged across all pulses in the scan. The duration of force was calculated as the time period between the onset and offset of a force pulse. The onset of a force pulse was the data sample at which the subject reached 5% of the peak force level of that particular pulse. The offset of a force pulse was the data sample at which the force being produced by the subject reduced to less than 5% of the peak force level required for that particular pulse. Reaction time was the difference in time between the stimulus onset and onset of the force pulse. The peak rate of change of force was the maximum of the first derivative of force from the force onset to when the force level reached the target acquisition force. Since there were 10 pulses per block and 4 blocks, this resulted in 40 pulses per scan. The average of these 40 values was used in the statistical analysis for each dependent measure respectively. A separate one factor (prediction level) repeated measures ANOVA was performed for each dependent measure (average reaction time per scan, average rate of change of force per scan, average of mean force per scan, and average duration of force per scan) using STATISTICA v6.1.

fMRI head motion analysis—The fMRI data were imported from the scanner and data processing was performed using the public domain software AFNI (http://afni.nimh.nih.gov/afni/). Motion detection and correction (3Dvolreg) were performed on each functional dataset of each subject. To be included in data analysis, the permitted head movement (peak to peak displacement) had to be less than a third of a voxel (voxel size =3.125 × 3.125 × 3mm) in any direction. All subjects met this strict criterion and were included in the data analysis.

Voxel-wise group analysis—The voxel-wise analysis identified regions of the brain that showed a significant change in BOLD signal across the three levels of predictability. We used a Gaussian filter with a FWHM of 3mm on each subject's motion corrected functional datasets. The signal within each scan of each subject was normalized by dividing the signal in each voxel recorded at each TR of the time series by the average signal in that voxel during the entire time series. Next, a multiple regression analysis was performed (3dDeconvolve) that calculated the task related regression coefficient between the expected hemodynamic response and the actual hemodynamic response obtained in each of the scans. A simulated hemodynamic response that corresponded to the time series of the 5 rest and 4 force task blocks was regressed to each of the functional datasets. Before group analyses, each subject's anatomical dataset was manually transformed to Talairach space using AFNI. Then, each subject's individual functional datasets were transformed to Talairach space using the normalized anatomical dataset as a template. All coordinates are reported in Talairach space, and in MNI coordinates based on the tal2icbm MATLAB algorithm (Laird et al., 2005).

A mixed-effect two-way ANOVA was then performed at the group level with the three levels of predictability as a fixed factor and subject as a random factor. In order to control for Type I error, a Monte Carlo simulation (AlphaSim in AFNI) was performed that provides a correction for the large number of tests performed during the group analysis. According to this simulation the number of voxels that make a cluster should be equal to 7 or more for a corrected p value of 0.05. The group map was threshholded to include voxels that had $p < 0.005$. According to the results of the AlphaSim simulation, clusters of activation with a volume size of 205 mm^3 or more (3.125 × 3.125× 3 × 7) were included in the group map. Anatomical guidelines from previously published literature were used to help identify each cluster of activation in the cortex (Mayka et al., 2006), basal ganglia (Prodoehl et al., 2008a), and cerebellum (Schmahmann et al., 2000).

Regions of interest analysis—To quantify the relation between prediction level and percent signal change, we also used a region of interest (ROI) analysis. Template masks containing these regions of the cortex, basal ganglia, and cerebellum were drawn a priori based

NIH-PA Author Manuscript

NIH-PA Author Manuscript

NIH-PA Author Manuscript

on templates regularly used in our laboratory (Mayka et al., 2006; Prodoehl et al., 2008a; Schmahmann et al., 2000) and were therefore independent of the voxel-wise results (Kriegeskorte et al., 2009). In addition to examining areas identified in the voxel-wise results, we also conducted an ROI analysis in external globus pallidus (GPe), internal globus pallidus (GPi), and subthalamic nucleus (STN). This analysis was performed to increase our confidence that these three areas of the basal ganglia did not scale with prediction. For calculating the percent signal change of each voxel, we first calculated the mean signal during the rest block of a scan and the mean signal during the force blocks of the same scan. Then, the difference in signal change during the force and rest blocks for each scan was calculated. The average percent signal change for the positive percent signal change voxels in each of the three predictability conditions was quantified (3dROIstats in AFNI). One-way repeated measures ANOVAs, with three prediction levels (20%, 40%, 80%) as the factor, were performed for percent signal change in GPe, GPi, and STN. The ANOVAs were interpreted as significant based on $p < 0.05$.

Results

Force output performance

In accordance with the design of the experiment, mean force did not change across the three levels of predictability (Figure 2A) [$F(2, 20) = 0.68$, $p > 0.05$]. Similarly, Figure 2B shows the mean duration of force was not different across the three levels of predictability [$F(2, 20) = 0.04$, $p > 0.05$]. These results confirm that any differences observed in the brain imaging analyses were not related to differences in either the magnitude or duration of force. Figure 2C shows that, consistent with the study hypothesis, mean reaction time reduced across the levels of predictability [$F(2, 20) = 10.83$, $p < 0.05$]. Figure 2D indicates that the rate of change of force increased with prediction level [$F(2, 20) = 19.13$, $p < 0.05$].

Voxel-wise fMRI group analysis

The voxel-wise group analysis identified several foci of activation located in the frontal lobe, parietal lobe, basal ganglia and cerebellum that showed significant differences in signal change across the three levels of predictability. Table 1 lists the co-ordinates in Talairach and MNI space of the centroid of activation of the significant cortical and subcortical regions. Figure 3A (top) displays activation in the left dorsolateral prefrontal cortex (DLPFC) located in the dorsal portion of area 46. Figure 3A (bottom) displays activation in the rostral (pre supplementary motor area, pre-SMA) and the caudal (SMA) portion of area 6. Activation clusters were observed in other areas of the cortex as well (not shown in Figure 3A, see Table 1). On the superior and lateral surface of the frontal lobe, activation in the region of the dorsal premotor cortex (PMd) was found bilaterally. Parietal lobe activation was localized to the right inferior parietal lobule (IPL) and bilateral precuneus (Table 1).

Figure 4A displays activation within subcortical areas. Figure 4A displays the rostrally located activation within the left caudate, and Figure 4B shows the cluster in left anterior putamen of the basal ganglia. In addition, the right anterior putamen (see Table 1) also showed a significant change in activity with prediction level (Figure 4A). Thalamic activation was found bilaterally in the ventrolateral subdivision of the thalamus (Table 1). Figure 4C illustrates activation within the left lobule V/VI and right lobule VI of the cerebellum. In addition, an activated cluster was also noted in the left and right lobule VIII of the cerebellum (Table 1).

Regions of interest analysis

The BOLD response was further examined using ROI analyses of percent signal change. Figure 3B illustrates the percent signal change results of the ROI analysis for the left DLPFC, pre-SMA and SMA and Figure 4B illustrates the percent signal change results for the left caudate,

NIH-PA Author Manuscript

NIH-PA Author Manuscript

NIH-PA Author Manuscript

left and right anterior putamen, left lobule V/VI and right lobule VI. An ROI analysis was also used to further confirm that other basal ganglia nuclei did not have a BOLD signal that changed across prediction level. Figure 5 shows that the BOLD signal in GPe, GPi, and STN did not change across prediction level. The statistical analysis supported Figure 5 [GPe: $F(2, 20) = 1.9$, $p = 0.17$; GPi: $F(2, 20) = 1.3$, $p = 0.27$; STN: $F(2, 20) = 0.8$, $p = 0.45$].

Discussion

This study used fMRI to examine the brain regions that mediate the prediction of grip force output. The findings demonstrate that in addition to the cortex, ventral thalamus, and cerebellum, anterior nuclei in the basal ganglia (caudate and anterior putamen) have a BOLD signal that increases with the level of grip force prediction. In contrast, posterior nuclei in the basal ganglia did not have a BOLD signal that scaled with the level of prediction. These findings provide new evidence that the basal ganglia are involved in the predictive scaling of precision grip force control. Further, the results show that it is the caudate and anterior putamen that modified their activation consistent with a role of the anterior basal ganglia nuclei in the planning aspects of grip force control (Prodoehl et al. 2009).

Predicting Grip Force Amplitude

When gripping and lifting an object of a constant weight, Schmitz and colleagues (2005) previously identified a network of activated brain areas which includes the contralateral motor cortex, PMd, cingulate motor area, SMA, cerebellum (lobules V, VI), IPL, and ventral thalamus (Schmitz et al., 2005). When the weight of the object is known to be constant, the amplitude of force that must be applied to lift the object is fully predictable. Schmitz and colleagues (2005) also found that when the weight is altered between two choices in a predictable manner compared to a constant weight, the left postcentral sulcus, left cerebellum (lobule VI), left thalamus, and left parietal operculum have an increased BOLD signal. The current study found that the BOLD signal parametrically increased with the prediction level in the SMA, left and right PMd, left DLPFC, right IPL, left and right precuneus, left and right thalamus, left cerebellum (lobules VI, VIII), and right cerebellum (Crus I and lobule VIII). Consistent with our hypothesis, we also found that the BOLD signal in left caudate, and left and right anterior putamen increased with the prediction level. While there are some differences in the regions identified between studies, there does appear to be general agreement that when predicting grip force amplitude, a network including PMd, SMA, cerebellum, IPL, and ventral thalamus are necessary to successfully execute sequences of grip force pulses that require prediction.

One of the main areas that differ between the current study and the study by Schmitz and colleagues (2005) is the basal ganglia. For instance, Schmitz and colleagues did not report any activation in the basal ganglia, even during the contrasts comparing grip and lift to baseline rest. The study by Schmitz and colleagues (2005) required subjects to grip and lift a heavy weight repeatedly without a large cognitive component to the task. In the current study, subjects had to maintain a specific rule about upcoming grip force amplitudes in memory, and this additional requirement may have required subjects to access working memory circuits (ie. DLPFC and caudate) that were not utilized during the task used by Schmitz and colleagues (2005). Also, our study was guided by visual feedback, whereas the study by Schmitz and colleagues blindfolded the subjects during the scanning protocol. It has been shown that providing visual feedback during a grip force task can increase BOLD fMRI signals in the basal ganglia (Vaillancourt et al., 2003). It should be pointed out that in our three visual feedback conditions the same level of visual stimulation was provided for each level of prediction, which suggests that visual feedback alone was an unlikely source to explain the current findings. Another possible factor to explain why we found basal ganglia activation and Schmitz and colleagues (2005) did not was the field strength of the magnet used in each study.

NIH-PA Author Manuscript

NIH-PA Author Manuscript

NIH-PA Author Manuscript

A 1.5T scanner was used by Schmitz and colleagues (2005) and it is established that BOLD signals are weaker at 1.5 T compared with 3T (Menon et al., 1998). Since the current study used a 3T scanner, basal ganglia activation may have been detected because of increased signal to noise ratio.

When the prediction level increased, we found that reaction time decreased and rate of change of force increased. One might suspect that the rate of change of force could have influenced the activity in the caudate and anterior putamen. Previously, our laboratory has designed experiments that specifically manipulated the rate of change of force (Prodoehl et al., 2008b; Vaillancourt et al., 2004). These two studies demonstrated that GPi and STN change in percent signal change when the rate of change of force is increased, whereas caudate, anterior putamen, posterior putamen, and GPe do not change in percent signal change with the rate of change of force. As such, since the current study found that anterior putamen and caudate increase in percent signal change with prediction level, the rate of change of force is an unlikely explanation for the current results.

Adequate grip force prediction may require holding predictive information in working memory and utilizing the predictive information in the programming of motor output. This is consistent with the parametrically increased BOLD scaling of areas seen in Table 1. Several types of memory have been discussed in relation to predictive grip force tasks. When humans lift objects they tend to scale fingertip forces according to the previous lift, and this has been referred to as sensorimotor memory (Johansson and Westling, 1984,1988b;Nowak et al., 2007;Quaney et al., 2003). Since the average force level and duration of force pulses was similar across the predictive conditions, we speculate that sensorimotor memory was most likely also similar across all three predictable conditions. Another type of memory is accessed when visual analysis of the object size and shape enable visuomotor transformations that facilitate memory for predictive grip force mechanisms (Gordon et al., 1991a;Jenmalm et al., 2000). An example of this in everyday life would be applying greater grip and load force to a carton of milk that has a greater volume of liquid than the same carton of milk with less liquid. In this example, prediction would occur whether the carton contains a large or small amount of liquid, and the level of memory would likely be the same. In the current study the target was visual and subjects likely used the visual feedback to facilitate memory circuits to predict grip force amplitude on subsequent force pulses. It could also be argued that when a greater number of predictions were required, working memory circuits were accessed to a greater extent. Indeed, the 40% and 80% conditions required additional cognitive functions such as rule retrieval in order to implement grip force predictions. It is therefore possible that the additional demands of rule retrieval enhanced the neuronal activity in areas involved in performing grip force prediction. It is also possible that other types of grip force prediction would not need to access memory circuits to the extent demanded in this study.

Previous studies have observed preparatory activity in the striatum (caudate and putamen) of monkeys prior to limb movements, and predictive information has been shown to influence single cell activity (Apicella et al., 1998; Jaeger et al., 1993). During self-timed movements a slow increase in putaminal activity has been observed in the monkey striatum hundreds of milliseconds prior to movement (Lee and Assad, 2003). Such preparatory activity may not underlie the current results for the putamen. In this experiment, the timing of all the force pulses was known in advance and was the same (every 3s) for each predictive condition. Thus, while preparatory activity for the timing of each pulse may well have occurred in the putamen in the current task, our results suggest the presence of specialized putaminal activity that was only seen when the upcoming grip force amplitude could be predicted. This anterior putaminal activity was absent when force amplitude prediction was not possible. Thus it seems unlikely that the anterior putaminal activity seen in our experiment was the same as the preparatory activity observed during self-timed movements (Lee and Assad, 2003). This point is further

NIH-PA Author Manuscript

NIH-PA Author Manuscript

NIH-PA Author Manuscript

supported by a study that examined alternating and equal intervals of either force or time. Pope and colleagues (2005) examined a task that required subjects to produce force pulses during four conditions that had: 1) equal temporal intervals and equal force, 2) alternating intervals and equal force, 3) equal intervals and alternating force, and 4) alternating intervals and alternating force. The condition that resulted in the greatest activity in the putamen was the condition that required alternating force, rather than alternating temporal intervals. The alternating force task required subjects to actively predict the force amplitude on each force pulse, and this finding is consistent with the hypothesis that the left anterior putamen is involved in actively predicting grip force amplitude.

In the present study, caudate and anterior putamen activity increased when a greater number of grip force predictions were implemented. A recent study which examined dopamine synthesis capacity using positron emission tomography and event-related fMRI suggests a differential role of the caudate and putamen during the performance of a working memory task (Landau et al., 2009). The authors found that both caudate and putamen activity increased with the working memory load. In addition, the authors found that caudate dopamine correlated positively with working memory capacity whereas putamen dopamine correlated positively with motor speed. The current findings cannot differentiate between different roles of the caudate and putamen in grip force prediction and future work is necessary to examine this interesting issue in more detail.

Planning and Parameterization Model of the Basal Ganglia

In addition to its role in the control of limb movements, there is emerging evidence from work in healthy individuals, as well as in individuals with diseases affecting the basal ganglia, that the basal ganglia play an important role in the control of precision grip force. Prodoehl and colleagues (2009) have recently proposed the hypothesis that anterior basal ganglia nuclei (anterior putamen, caudate and GPe) are important in regulating specific planning aspects related to precision grip force control, and that posterior basal ganglia nuclei (GPi and STN) are important in regulating the parameterization of precision grip force control. This hypothesis was based on several experimental observations which centered on the parametric scaling of activation within specific nuclei of the basal ganglia during precision gripping tasks (Prodoehl et al., 2008b; Spraker et al., 2007; Vaillancourt et al., 2004; Vaillancourt et al., 2007). The general model suggested by Prodoehl and colleagues (2009) is that anterior nuclei in the basal ganglia have a BOLD signal that increases when the selection and prediction of force amplitude occurs during the grip task. On the other hand, posterior nuclei have a BOLD signal that scales with the rate of change of force and overall amplitude of grip force exerted during the task. The rate of change of force varied between 150-225 %MVC/s in the current study (Figure 2), and previous evidence indicates that the percent signal change does not change with the rate of change of force in this range (see Figure 6, Prodoehl et al. 2008b).

The current findings provide expanded evidence in support of the planning and parameterization model because both caudate and anterior putamen (Figure 4) had an increased BOLD signal when the prediction level of the grip force task increased. Consistent with this model, other basal ganglia nuclei proposed to regulate the parameterization of grip force did not have a BOLD signal that scaled with prediction level (Figure 5). It remains to be seen if the caudate and anterior putamen have different roles in grip force prediction, and what this might mean for force prediction deficits in individuals with abnormal basal ganglia function such as Parkinson's disease.

Relation between Basal Ganglia, Cerebellum, and Parietal-Frontal Circuits of Grasping

The control of grasping requires precise coordination of fingertip forces (Castiello, 2005; Johansson and Westling, 1984, 1988a). It has been proposed that two anatomically segregated

NIH-PA Author Manuscript

NIH-PA Author Manuscript

NIH-PA Author Manuscript

parieto-frontal circuits exist for the control of reaching and grasping: a dorsolateral circuit controlling the grasp component, consisting of an anterior intraparietal (AIP) area connected to the rostral part of the ventral premotor cortex (PMv), and a dorsomedial circuit controlling the reaching component, consisting of the anterior portion of the occipito-parietal sulcus (area V6A) and the caudal dorsal premotor cortex (PMd) (Galletti et al., 2003; Tanne-Gariepy et al., 2002). However, it should be noted that there may not be a strict dichotomy between circuitry controlling the reach and grasp components. In an analysis of the changes in effective connectivity in the occipito-parieto-frontal network during a visually guided reach and grasp task, Grol et al. (2007) suggest that contributions to the dorsolateral and dorsomedial circuits are a function of the degree of on-line control required by the task related in part to the object size and width. Consistent with this hypothesis related to the degree of on-line control, our laboratory has previously shown that the level of visual information modulates the activity in dorsal premotor cortex (PMd) and PMv during precision grip force control (Vaillancourt et al., 2006). In the current study, it was found that PMd increased with the level of prediction, but while PMv was active during the task, the activity did not increase with the level of grip force prediction. Our findings are different from a recent study using TMS. Dafotakis and colleagues (2008) studied the effects of single pulse TMS on primary motor cortex, PMv, and AIP. The authors found that TMS over PMv interfered with the predictive scaling of grip forces according to the most recent lift when applied at the time of peak grasp aperture. TMS over AIP and primary motor cortex did not alter the predictive scaling of grip force. One of the main differences between the current study and the study by Dafotakis and colleagues (2008) is that we used a visually-guided grip force task, and this may have increased the level of on-line control necessary in the task thereby altering which part of the grasping network was involved in predicting force output (Grol et al., 2007; Vaillancourt et al., 2003).

The output nuclei of the basal ganglia, and also the cerebellum, have shown clear anatomical connectivity with two key nodes controlling grasping, namely AIP and PMv. PMv is the target of output from the GPi via the thalamus (Hoover and Strick, 1993; Middleton and Strick, 2000), and AIP receives a projection, via the thalamus, from neurons located in the caudal two thirds of the substantia nigra pars reticulata. In regards to the cerebellum, AIP is the target of cerebellar output via the thalamus (Clower et al., 2005), and PMv receives a projection from the dentate via the cerebellum (Middleton and Strick, 2000). Specifically, AIP receives a broadly distributed as well as a focal projection from the dentate nucleus of the cerebellum which forms an output channel via the thalamus to AIP. In the current study, we found right and left lobule VI, left and right lobule VIII, right crus I, and left lobule V increased activation with the level of grip force prediction. In a study of grip force corrections, it was found that the right cerebellum increased activity when the grip force was too high for the unexpected lighter object (Jenmalm et al., 2006). It was previously suggested that one possible role of the cerebellum may be related to the anticipatory and reactive aspects of disturbances in grip behavior (Serrien and Wiesendanger, 1999). Thus, the current findings on grip force prediction combined with those of Jenmalm and colleagues (2006) provides further empirical support for this hypothesis.

In summary, this study has shown that anterior nuclei of the basal ganglia are involved in the regulation of grip force prediction. These findings are consistent with the Planning and Parameterization Model of the Basal Ganglia (Prodoehl et al., 2009). In the context of the literature on grasping, the current study indicates that in addition to the well-established parieto-frontal circuit, specific areas of the basal ganglia and cerebellum also regulate components of grip force control. As such, the current findings are consistent with the emerging viewpoint that grasping may be viewed as a behavior that is regulated by a large motor network in the cortex and in subcortical structures.

NIH-PA Author Manuscript

NIH-PA Author Manuscript

NIH-PA Author Manuscript

Acknowledgments

This research was supported in part by grants from the National Institutes of Health (R01NS52318, R01NS58487, R01NS28127, R01NS40902, F32MH83424). We thank Mike Flannery and Hagai Ganin for assistance with data collection.

References

Apicella P, Ravel S, Sardo P, Legallet E. Influence of predictive information on responses of tonically active neurons in the monkey striatum. J Neurophysiol 1998;80:3341–3344. [PubMed: 9862929]

Castiello U. The neuroscience of grasping. Nat Rev Neurosci 2005;6:726–736. [PubMed: 16100518]

Clower DM, Dum RP, Strick PL. Basal ganglia and cerebellar inputs to 'AIP'. Cereb Cortex 2005;15:913–920. [PubMed: 15459083]

Dafotakis M, Sparing R, Eickhoff SB, Fink GR, Nowak DA. On the role of the ventral premotor cortex and anterior intraparietal area for predictive and reactive scaling of grip force. Brain Res 2008;1228:73–80. [PubMed: 18601912]

Dai TH, Liu JZ, Sahgal V, Brown RW, Yue GH. Relationship between muscle output and functional MRI-measured brain activation. Exp Brain Res 2001;140:290–300. [PubMed: 11681304]

Danion F, Sarlegna FR. Can the human brain predict the consequences of arm movement corrections when transporting an object? Hints from grip force adjustments. J Neurosci 2007;27:12839–12843. [PubMed: 18032655]

Flanagan JR, King S, Wolpert DM, Johansson RS. Sensorimotor prediction and memory in object manipulation. Can J Exp Psychol 2001;55:87–95. [PubMed: 11433790]

Forssberg H, Eliasson AC, Kinoshita H, Johansson RS, Westling G. Development of human precision grip. I: Basic coordination of force. Exp Brain Res 1991;85:451–457. [PubMed: 1893993]

Galletti C, Kutz DF, Gamberini M, Breveglieri R, Fattori P. Role of the medial parieto-occipital cortex in the control of reaching and grasping movements. Exp Brain Res 2003;153:158–170. [PubMed: 14517595]

Gordon AM, Forssberg H, Johansson RS, Westling G. Integration of sensory information during the programming of precision grip: comments on the contributions of size cues. Exp Brain Res 1991a; 85:226–229. [PubMed: 1884761]

Gordon AM, Forssberg H, Johansson RS, Westling G. Visual size cues in the programming of manipulative forces during precision grip. Exp Brain Res 1991b;83:477–482. [PubMed: 2026190]

Grol MJ, Majdandzic J, Stephan KE, Verhagen L, Dijkerman HC, Bekkering H, Verstraten FA, Toni I. Parieto-frontal connectivity during visually guided grasping. J Neurosci 2007;27:11877–11887. [PubMed: 17978028]

Hick WE. On the rate of gain of information. Quart. J. Exp. Psychol 1952;4:11–26.

Hoover JE, Strick PL. Multiple output channels in the basal ganglia. Science 1993;259:819–821. [PubMed: 7679223]

Hyman R. Stimulus information as a determinant of reaction time. J. Exp. Psychol 1953;45:188–196. [PubMed: 13052851]

Jaeger D, Gilman S, Aldridge JW. Primate basal ganglia activity in a precued reaching task: preparation for movement. Exp Brain Res 1993;95:51–64. [PubMed: 8405253]

Jenmalm P, Dahlstedt S, Johansson RS. Visual and tactile information about object-curvature control fingertip forces and grasp kinematics in human dexterous manipulation. J Neurophysiol 2000;84:2984–2997. [PubMed: 11110826]

Jenmalm P, Schmitz C, Forssberg H, Ehrsson HH. Lighter or heavier than predicted: neural correlates of corrective mechanisms during erroneously programmed lifts. J Neurosci 2006;26:9015–9021. [PubMed: 16943559]

Johansson RS, Cole KJ. Grasp stability during manipulative actions. Can J Physiol Pharmacol 1994;72:511–524. [PubMed: 7954081]

Johansson RS, Westling G. Roles of glabrous skin receptors and sensorimotor memory in automatic control of precision grip when lifting rougher or more slippery objects. Exp Brain Res 1984;56:550–564. [PubMed: 6499981]

NIH-PA Author Manuscript

NIH-PA Author Manuscript

NIH-PA Author Manuscript

Johansson RS, Westling G. Coordinated isometric muscle commands adequately and erroneously programmed for the weight during lifting task with precison grip. Experimental Brain Research 1988a;71:59–71.

Johansson RS, Westling G. Programmed and triggered actions to rapid load changes during precision grip. Exp Brain Res 1988b;71:72–86. [PubMed: 3416959]

Kriegeskorte N, Simmons WK, Bellgowan PS, Baker CI. Circular analysis in systems neuroscience: the dangers of double dipping. Nat Neurosci 2009;12:535–540. [PubMed: 19396166]

Laird AR, McMillan KM, Lancaster JL, Kochunov P, Turkeltaub PE, Pardo JV, Fox PT. A comparison of label-based review and ALE meta-analysis in the Stroop task. Hum Brain Mapp 2005;25:6–21. [PubMed: 15846823]

Landau SM, Lal R, O'Neil JP, Baker S, Jagust WJ. Striatal dopamine and working memory. Cereb Cortex 2009;19:445–454. [PubMed: 18550595]

Lee IH, Assad JA. Putaminal activity for simple reactions or self-timed movements. J Neurophysiol 2003;89:2528–2537. [PubMed: 12611988]

Mayka MA, Corcos DM, Leurgans SE, Vaillancourt DE. Three-dimensional locations and boundaries of motor and premotor cortices as defined by functional brain imaging: a meta-analysis. Neuroimage 2006;31:1453–1474. [PubMed: 16571375]

Menon V, Glover GH, Pfefferbaum A. Differential activation of dorsal basal ganglia during externally and self paced sequences of arm movements. Neuroreport 1998;9:1567–1573. [PubMed: 9631468]

Middleton FA, Strick PL. Basal ganglia and cerebellar loops: motor and cognitive circuits. Brain Res Brain Res Rev 2000;31:236–250. [PubMed: 10719151]

Nowak DA, Koupan C, Hermsdorfer J. Formation and decay of sensorimotor and associative memory in object lifting. Eur J Appl Physiol 2007;100:719–726. [PubMed: 17503069]

Pope P, Wing AM, Praamstra P, Miall RC. Force related activations in rhythmic sequence production. Neuroimage 2005;27:909–918. [PubMed: 15993627]

Prodoehl J, Corcos DM, Vaillancourt DE. Basal ganglia mechanisms underlying precision grip force control. Neurosci Biobehav Rev 2009;33:900–908. [PubMed: 19428499]

Prodoehl J, Yu H, Little DM, Abraham I, Vaillancourt DE. Region of interest template for the human basal ganglia: comparing EPI and standardized space approaches. Neuroimage 2008a;39:956–965. [PubMed: 17988895]

Prodoehl J, Yu H, Wasson P, Corcos DM, Vaillancourt DE. Effects of visual and auditory feedback on sensorimotor circuits in the basal ganglia. Journal of Neurophysiology 2008b;99:3042–3051. [PubMed: 18287549]

Quaney BM, Rotella DL, Peterson C, Cole KJ. Sensorimotor memory for fingertip forces: evidence for a task-independent motor memory. J Neurosci 2003;23:1981–1986. [PubMed: 12629204]

Schmahmann, JD.; Doyon, J.; Toga, AW.; Petrides, M.; Evans, AC. MRI Atlas of the human cerebellum. Academic press; San Diego: 2000.

Schmitz C, Jenmalm P, Ehrsson HH, Forssberg H. Brain activity during predictable and unpredictable weight changes when lifting objects. J Neurophysiol 2005;93:1498–1509. [PubMed: 15385599]

Serrien DJ, Wiesendanger M. Role of the cerebellum in tuning anticipatory and reactive grip force responses. J Cogn Neurosci 1999;11:672–681. [PubMed: 10601748]

Spraker MB, Yu H, Corcos DM, Vaillancourt DE. Role of individual Basal Ganglia nuclei in force amplitude generation. J Neurophysiol 2007;98:821–834. [PubMed: 17567775]

Tanne-Gariepy J, Rouiller EM, Boussaoud D. Parietal inputs to dorsal versus ventral premotor areas in the macaque monkey: evidence for largely segregated visuomotor pathways. Exp Brain Res 2002;145:91–103. [PubMed: 12070749]

Thulborn KR, Shen GX. An integrated head immobilization system and high-performance RF coil for fMRI of visual paradigms at 1.5 T. J Magn Reson 1999;139:26–34. [PubMed: 10388581]

Vaillancourt DE, Mayka MA, Corcos DM. Intermittent visuomotor processing in the human cerebellum, parietal cortex, and premotor cortex. J Neurophysiol 2006;95:922–931. [PubMed: 16267114]

Vaillancourt DE, Mayka MA, Thulborn KR, Corcos DM. Subthalamic nucleus and internal globus pallidus scale with the rate of change of force production in humans. Neuroimage 2004;23:175–186. [PubMed: 15325364]

NIH-PA Author Manuscript

NIH-PA Author Manuscript

NIH-PA Author Manuscript

Vaillancourt DE, Thulborn KR, Corcos DM. Neural basis for the processes that underlie visually guided and internally guided force control in humans. J Neurophysiol 2003;90:3330–3340. [PubMed: 12840082]

Vaillancourt DE, Yu H, Mayka MA, Corcos DM. Role of the basal ganglia and frontal cortex in selecting and producing internally guided force pulses. Neuroimage 2007;36:793–803. [PubMed: 17451971]

NIH-PA Author Manuscript

NIH-PA Author Manuscript

NIH-PA Author Manuscript

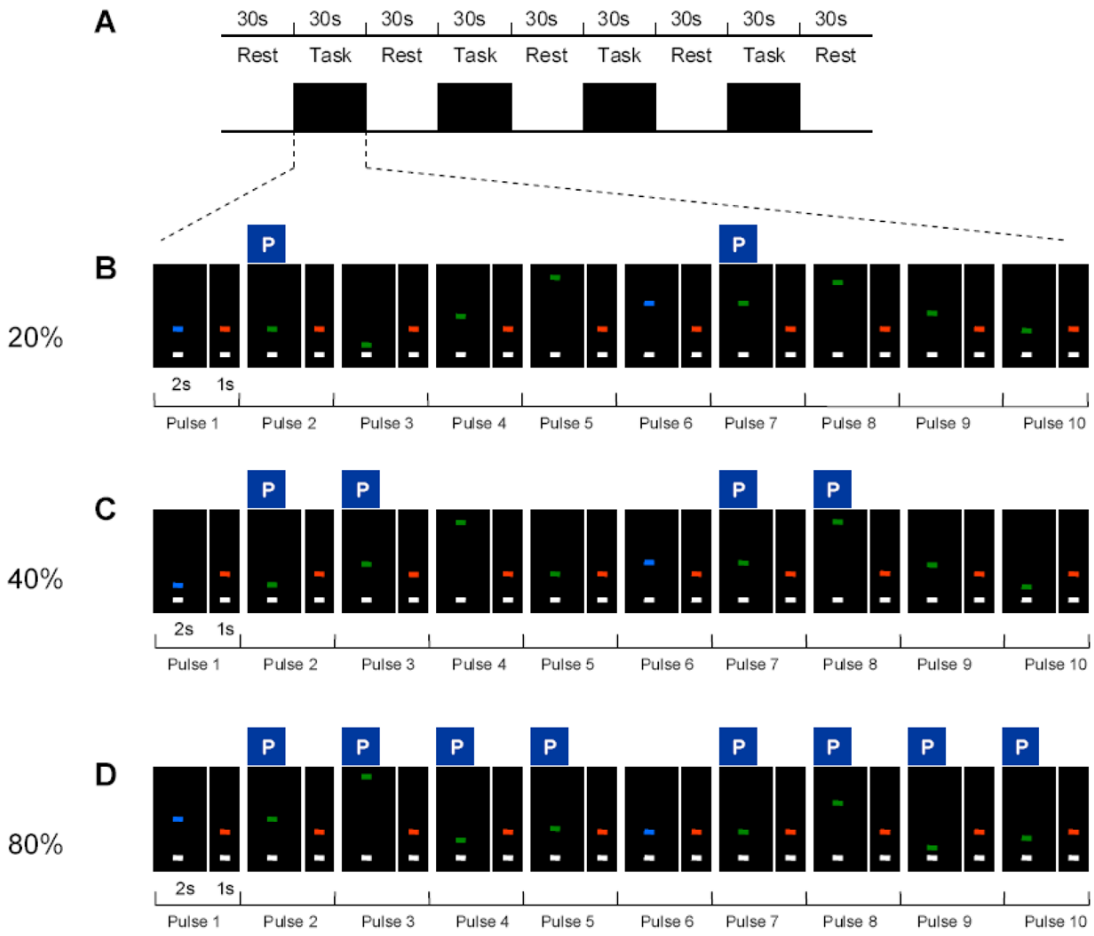

Figure 1.

Experimental design for the prediction task. **A**, shows the general schematic of the experimental block design which was the same in each scan. **B-D**, the sequence of ten force pulses (each with 2s of force contraction and 1s of rest) within a task block in the 20% level of predictability, 40% level of predictability, and 80% level of predictability. The P above each respective pulse indicates which pulses were predictable during each predictability condition. Note the target bars are blue for the first and sixth reference pulses and green for the other pulses. The target force levels for predictable pulses appear at amplitude levels determined by the rule governing each level of predictability previously learned by the subject.

NIH-PA Author Manuscript

NIH-PA Author Manuscript

NIH-PA Author Manuscript

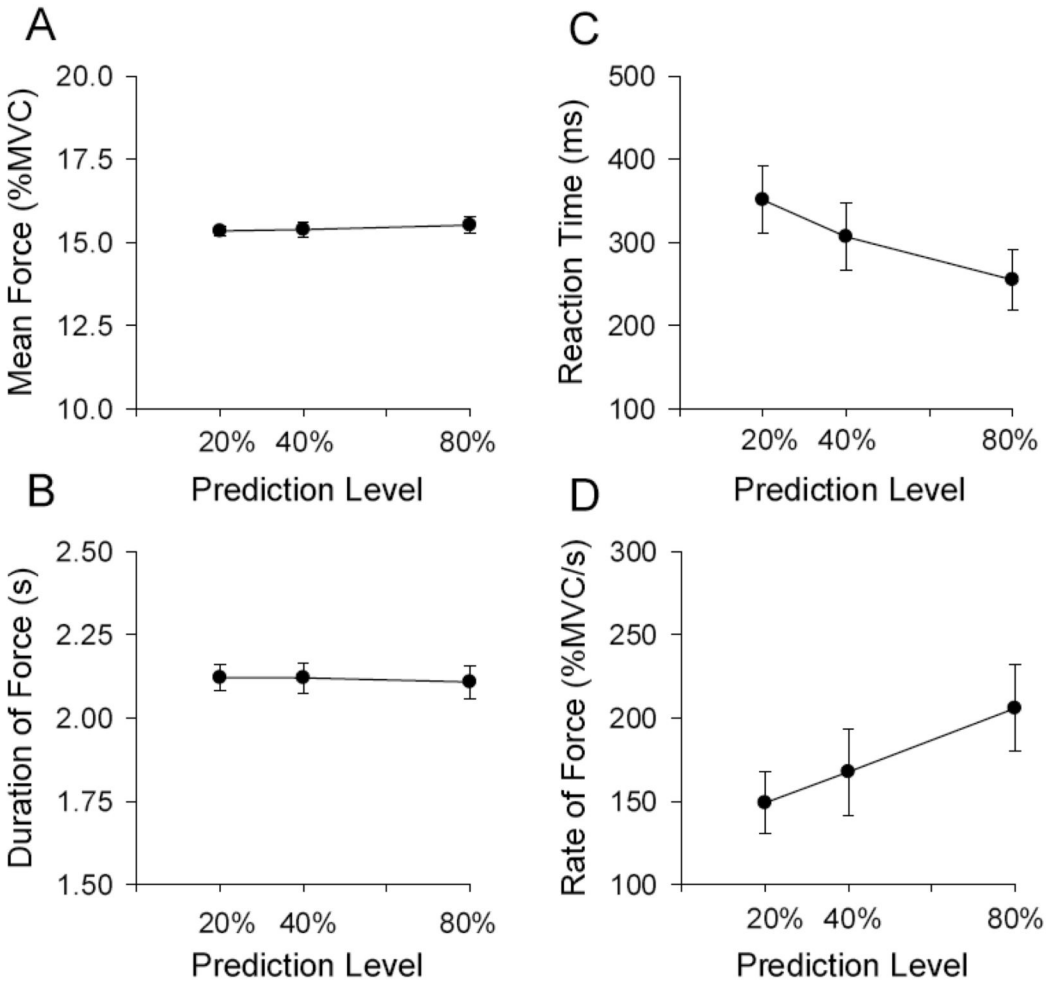

Figure 2.

Behavioral force output performance. **A**, shows the group mean force output, **B** shows the group mean duration of force, **C** shows the group mean reaction time, and **D** shows the rate of change of force. Each data in Figure 2 represents the average across the 40 pulses (10 pulses in 4 blocks) for each subject, which was then averaged across the 11 subjects in the study. The standard error of the mean is shown at each prediction level.

NIH-PA Author Manuscript
NIH-PA Author Manuscript
NIH-PA Author Manuscript

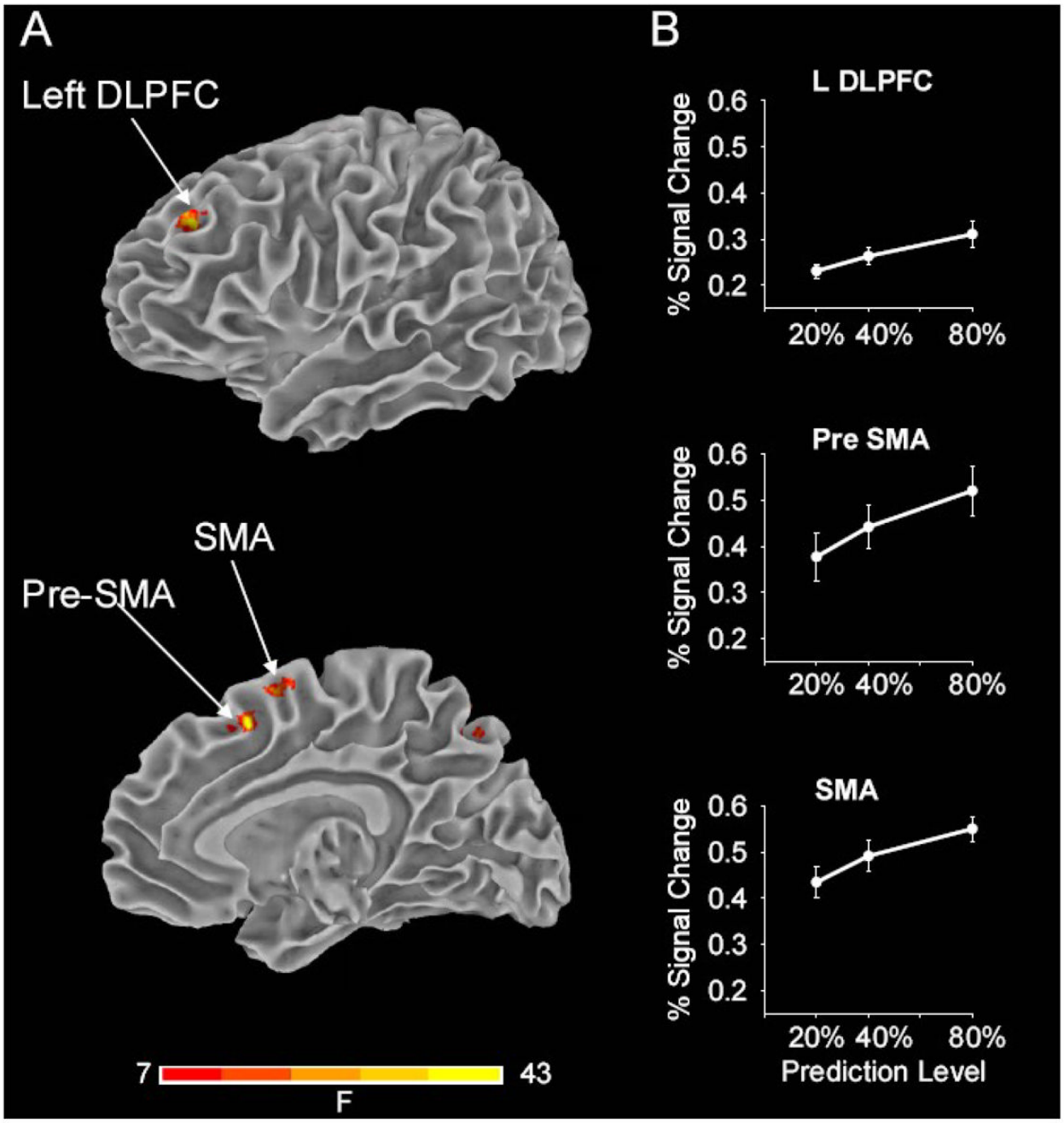

Figure 3.

Brain imaging results in the cortex across prediction level. **A**, displays the results from the voxel-wise group analysis showing task related activity in cortical areas that include left dorsolateral prefrontal cortex (DLPFC), pre-supplementary motor area (pre-SMA) and SMA. The group activation threshold is at $p < 0.05$ (corrected). The complete results from the voxel-wise analysis are presented in Table 1. **B**, shows results from the ROI analysis with percent signal change in the left DLPFC, pre-SMA and SMA. These cortical areas form part of the network that scaled significantly in activation with increases in the level of predictability. The standard error of the mean is shown at each prediction level.

NIH-PA Author Manuscript
NIH-PA Author Manuscript
NIH-PA Author Manuscript

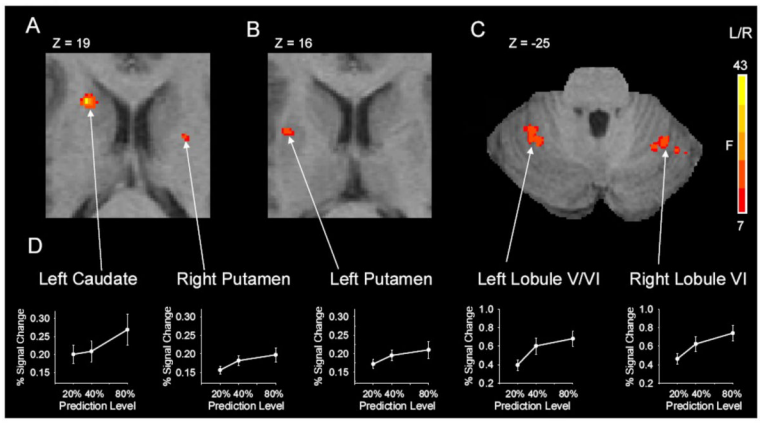

Figure 4.

Subcortical brain imaging results across prediction level. **A-C**, displays the results from the voxel-wise group analysis showing task related activity in subcortical areas that include left caudate, left and right putamen, left and right lobule VI of the cerebellum. The complete results are shown in Table 1. **D**, depicts results from the ROI analysis with percent signal change in these same areas. These subcortical areas form part of the network that scaled significantly in activation across the levels of predictability. The standard error of the mean is shown at each prediction level.

NIH-PA Author Manuscript

NIH-PA Author Manuscript

NIH-PA Author Manuscript

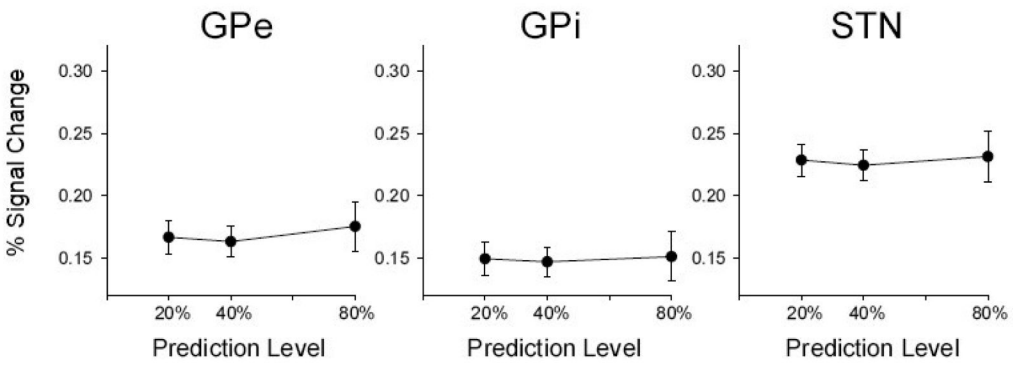

Figure 5.

Posterior basal ganglia activation across prediction level. Displays the results from the ROI analysis with percent signal change as the dependent measure. These subcortical areas of the basal ganglia did not change in signal intensity across the grip prediction level. External globus pallidus (GPe), internal globus pallidus (GPi), and subthalamic nucleus (STN) are shown. The standard error of the mean is shown at each prediction level.

NIH-PA Author Manuscript NIH-PA Author Manuscript NIH-PA Author Manuscript

Table 1

Results from voxel-wise analysis

Region		Center of Mass from Voxel-wise					
		Talairach Coordinates			MNI Coordinates		
		RL	AP	IS	RL	AP	IS
Pre-SMA		3.6	9.8	49.2	5.3	15.8	49.4
SMA		1.0	3.0	57.0	2.6	9.2	58.7
DLPFC	L	−31.7	41.2	32.7	−32.7	47.3	28.8
PMd	L	−21.1	−2.5	51.0	−21.0	2.8	52.8
	R	26.6	5.2	55.9	29.9	11.6	57.0
IPL	R	39.9	−46.5	47.3	44.3	−43.7	51.8
Precuneus	L	−7.2	−71.2	43.8	−6.0	−70.4	50.8
	R	18.8	−66.4	47.8	21.8	−64.8	54.4
Thalamus	L	−16.3	−12.0	6.0	−16.2	−11.1	3.7
	R	14.2	−13.3	6.3	16.4	−12.3	3.8
Anterior Putamen	L	−25.0	−4.0	16.0	−25.5	−1.9	14.2
	R	21.0	0.0	20.0	23.7	3.0	17.7
Caudate	L	−15.9	8.7	21.5	−15.8	12.1	19.1
Crus I	R	43.3	−55.2	−28.9	47.3	−59.4	−31.9
Lobule V/VI	L	−32.6	−43.7	−27.2	−33.8	−47.6	−30.0
Lobule VI	R	32.2	−54.2	−21.4	35.5	−57.8	−23.5
Lobule VIII	L	−17.1	−49.4	−44.0	−17.4	−54.9	−48.3
	R	21.9	−46.7	−43.3	24.3	−51.8	−48.3

RL (right left), AP (anterior posterior), IS (inferior superior) coordinates represent the location of the center of mass of the activated cluster within Talairach and MNI space; Abbreviations from top: R, right hemisphere; L, left hemisphere; pre-SMA, pre-supplementary motor area; SMA, supplementary motor area; DLPFC, dorsolateral prefrontal cortex; PMd, dorsal premotor cortex; IPL, inferior parietal lobe; crus I, lobule V/VI and lobule VIII are regions within the cerebellum.